Numerical Simulation of Stage Jettisoning of a Two-Stage Rocket with Different Separation Distances

R. Balasubramanian,
K. Anandhanarayanan,
R. Krishnamurthy & D. Chakraborty

Journal of The Institution of Engineers (India): Series C
Mechanical, Production, Aerospace and Marine Engineering

ISSN 2250-0545

J. Inst. Eng. India Ser. C
DOI 10.1007/s40032-012-0036-y

Springer

J. Inst. Eng. India Ser. C
DOI 10.1007/s40032-012-0036-y

ORIGINAL CONTRIBUTION

Numerical Simulation of Stage Jettisoning of a Two-Stage Rocket with Different Separation Distances

R. Balasubramanian · K. Anandhanarayanan · R. Krishnamurthy · D. Chakraborty

Received: 22 December 2011 / Accepted: 26 July 2012

Abstract CFD simulations were carried out to evaluate the flow field during the jettisoning process of a two-stage rocket using an inhouse developed RANS code. Two simulations with stage separation distances of 500 mm and 1,000 mm were considered for simulation. For the 500 mm case, there was a severe 'jet-upstream' flow interaction which resulted in an upstream flow separation and hence can cause large drag rise. However, there was no such observation of flow separation anywhere on the upper stage for the 1,000 mm case. A study was carried out to evaluate the effect of spatial order of accuracy for modelling the governing Reynolds Averaged Navier–Stokes (RANS) equations on the simulation results.

Keywords Stage separation distance · CFD simulations · Two stage rocket · Safe distance · Evaluation

Introduction

During stage separation of a two stage rocket (TSR), firing of the upper stage rocket motor in the proximity of the spent lower-stage can create instability to the upper stage if the distance between the two stages is lower than a critical. The critical or safe distance henceforth mentioned is defined to be the 'distance between the upper stage nozzle exit and the dome-crown of the spent lower stage'. To design the jettisoning process sequence and the precise instant to fire the upper stage rocket motor, it is necessary to understand the flow field during the jettisoning process. The forces and moments will provide necessary inputs for the separation dynamics study.

Experimental methods may lead to a safe and successful separation [1–4] but such methods are expensive and time consuming. Other than experimental tests, semi empirical and numerical methods have been widely used in this area. Kumar et al. [5] presented a simple and effective analytical model for estimating the forces and moments experienced by the inter-stage barrel due to impingement of jet exhaust during hot stage separation of a launch vehicle using CFD data and Newtonian impact theory.

With the advent of robust numerical technique, faster computer, CFD is playing an important role in estimating the forces and moments for separation dynamics study. Bunning et al. [6] and Liever [7] described the use of several CFD methods for stage separation aerodynamics of hyper X separation from Peagasus launch vehicle. Unsteady effects, aerodynamic database extrapolation and differences between wind tunnel and flight environments were greatly described. Mirzaei et al. [8] presented RANS calculation with RNG K-epsilon model for the separation of multi stage aerospace vehicle and studied the external flow-jet flow interaction around the body components. Paglia et al. [9] presented the CFD analysis of separation process of VEGA launch vehicle using commercial CFD solver fluent. Zhang and Zhao [10] presented the computational studies of stage separation process using unstructured chimera grid. Pamadi et al. [11] described the generation of aerodynamic data base through wind tunnel test program and CFD methods using OVERFLOW code [12]. Wang et al. [13] studied the variation of flow field and aerodynamic coefficient for various separation distances by using a series of static and dynamic viscous simulations and their numerical results for $M = 3.0$ was compared with the experimental data.

R. Balasubramanian (✉) · K. Anandhanarayanan · R. Krishnamurthy · D. Chakraborty
CFD Division, Defence Research and Development Laboratory, Hyderabad, India
e-mail: bals.cfd@gmail.com

Published online: 13 November 2012

In the present study, the inter-stage zone of the TSR considered is fully closed. As the ambient flight condition of two-stage rocket at the time of stage separation is less dense with the flow interactions expected to be complex, CFD is the only viable option for studying the stage separation of the TSR and wind tunnel experiments require enormous effort for the problem set-up and hence very difficult to perform.

Hence CFD simulations were carried out to determine the safe separation distance. Since the dynamics of the flow is strictly governed by the separation distance with complex interplay of jet plume with free stream air, it is necessary to simulate the flow field for the coupled jet-air mixture over the full geometry involving the upper-stage and part of the lower stage. For the present analysis, two critical distances, viz., 500 and 1,000 mm were considered for simulations. compressible Euler-Reynolds averaged Navier–Stokes [14] (CERANS©) and AUTOmatic Elliptic GRID generator [15] (AUTOELGRID©) codes were used for the CFD analysis and the CLUSTER-32 system of DRDL was used for the computations.

Grid Generation

The upper stage of TSR is a blunt-cone-cylinder-flare configuration with a rocket motor nozzle being located at the stage end. The lower stage consists of a cylinder having its upper surface covered by a dome with a part of cylinder-skirt protruding forward to the dome-crown. Structured multiblock grids have been generated for the TSR geometry using AUTOELGRID, which is an inhouse developed automatic elliptic grid generator based on the Sorenson–Steger method. Since the geometry is axisymmetrical, initially a two dimensional grid was generated and rotated in the azimuthal direction to obtain the three dimensional grid. The grid consisted of four blocks, namely, the external, inter-stage space, nozzle and base-cavity zone (Figs. 1, 2). For the case 1 with a distance of 500 mm, the grid size used is about 0.48 million direction and for the case 2 having 1,000 mm, the grid size is about 0.56 million. The number of grid points in the azimuth direction is 65. Sufficient near wall clustering had been provided to resolve the boundary layer. Figures 1 and 2 show the grids used for the two distances in a symmetry plane.

Flowsolver Details and Flow Conditions

CERANS is a three dimensional grid-format-independent compressible viscous flow solver which solves the governing compressible RANS equations in a finite-volume framework on sequential and parallel computers. The

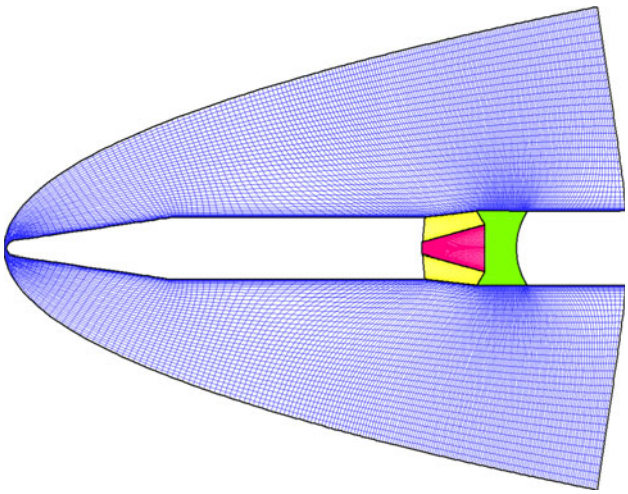

Fig. 1 Grid in symmetry plane for separation distance of 500 mm

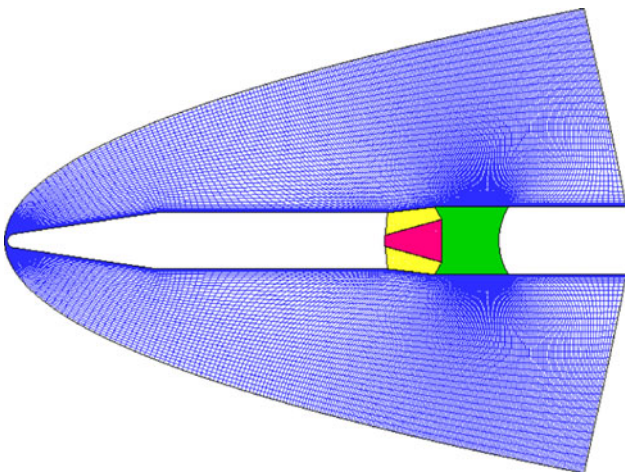

Fig. 2 Grid in symmetry plane for separation distance of 1,000 mm

interfacial numerical fluxes for the mean flow equations were evaluated using AUSM-PW flux formulae for the convective fluxes and central differencing for the diffusive fluxes. Second order spatial accuracy was used for evaluating the mean flow fluxes and Barth's min–max slope limiter was used to preserve monotonicity in regions of discontinuities. The one equation Spalart-Allmaras turbulence model had been used for addressing the closure problem. A robust reliable blended universal law of the wall [16] with compressibility and heat transfer correction had been used for modelling the near wall flow.

The free stream conditions of the TSR corresponding to a flight altitude of about 26.5 km (Indian standard atmosphere) and the jet conditions at the nozzle throat considered for CFD analysis are given in Table 1.

For the present simulations, the ratio of specific heats is held constant and the value of 1.233 for jet had been used throughout. The gas constant considered for the entire flow field is that of the jet, which is 319.77 J/kg-K. As CERANS

Table 1 Flow conditions for the TSR

Domain	Mach no. M_∞	Angle of attack (°)	Pressure (N/m^2)	Temperature (K)
Freestream	6.08	0	1,966	223.0
Jet	1.00	0	2,720,210	3,134.4

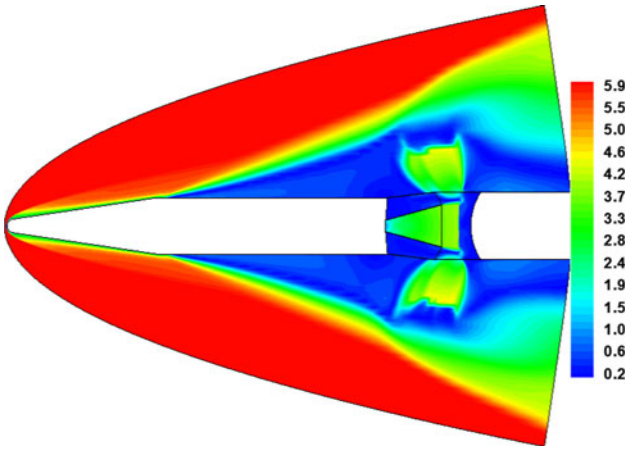

Fig. 3 Mach contours for separation distance of 500 mm

cannot handle gas decomposition, the free stream flow is assumed chemically frozen and is considered as perfect gas with the physical state purely governed by its gas dynamic behaviour only. For the present simulations, global minimum time step had been used for temporal evolution.

Stage Jettisoning of the Rocket

Flow simulations were carried out for the two distances namely, 500 and 1,000 mm. The results of flow simulation for 500 mm case are shown from Figs. 3, 4, and 5. Figure 3 shows the Mach contours and Fig. 4 shows the temperature (T/T_∞) contours. These contours show the detached bow shock ahead of the upper stage nose, a strong shock ahead of the lower stage dome due to the jet exhaust, a zone of flow separation over the upper stage cylinder, the Mach disc structure at the jet escape zone and a dead-air zone in the base-cavity region. The temperature had almost crimsoned to the stagnation temperature of jet in the base-cavity zone. This is expected due to the fact that the simulations were carried out with a constant ratio of specific heats.

The jet flow had to make an almost 'U' turn close to 180° at the stage-opening gap during its escape route to the external domain. This is achieved by jet traversing through the dome shock and a bounce back from the constricted cylindrical upstream shroud protrusion ahead of dome. A severe 'jet-upstream' flow interaction had taken place due to large momentum of flow in the transverse direction

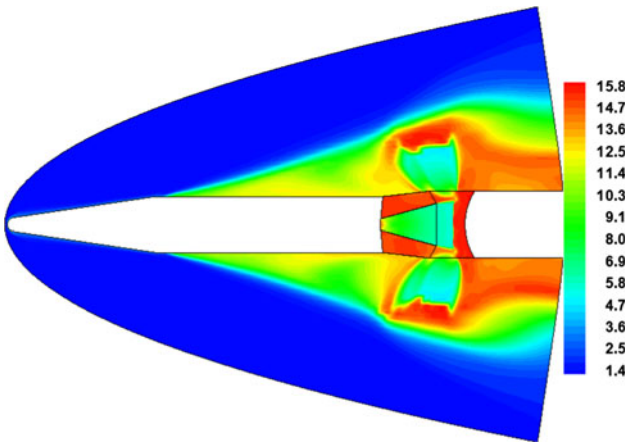

Fig. 4 Temperature contours (T/T_∞) for separation distance of 500 mm

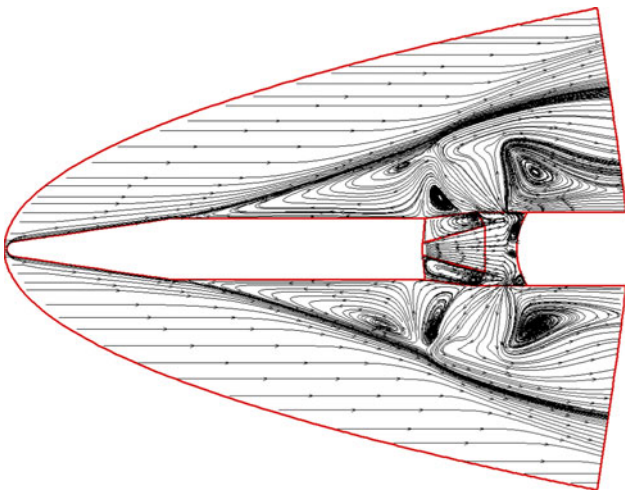

Fig. 5 Streamline pattern for separation distance of 500 mm

forming a distinctly visible Mach disc which is obstructing the external flow almost at 120° to it thereby resulting in a very large upstream flow separation. It can be seen that the extent of separation had reached the cone-cylinder shoulder junction. The streamline patterns shown in Fig. 5 depict several recirculation zones. It can be easily understood that these patterns are due to the large shear flows at several pockets of the domain contributed by various factors such as the direction of jet flow into the upstream, shape of the dome along with its upstream cylindrical extension, the separation distance, trapped dead air zones and the Mach disc. Also, due to large momentum of the jet in the traverse direction, a large recirculation zone had been formed downstream of the Mach disc along the axial direction.

The huge flow separation on the cylindrical portion of the upper stage as a result of 'jet-upstream' flow interaction can decelerate the TSR due to large increase in the drag force.

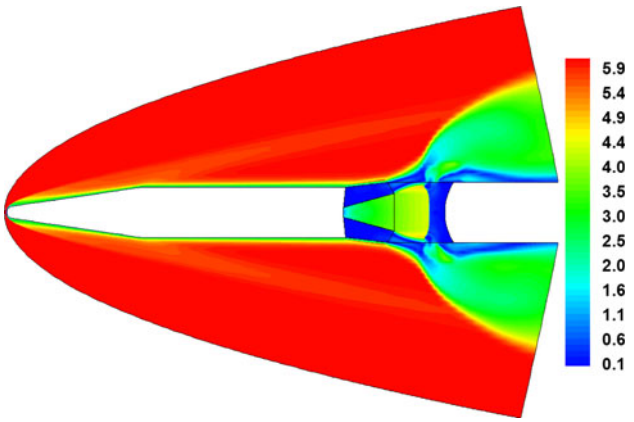

Fig. 6 Mach contours for separation distance of 1,000 mm

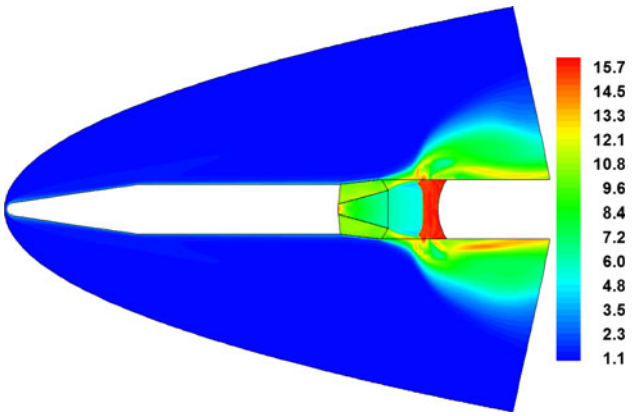

Fig. 7 Temperature contours (T/T_∞) for separation distance of 1,000 mm

The flow simulation at 1,000 mm stage separation distance had revealed an entirely different picture from that of the 500 mm. Figures 6 and 7 depict the Mach contours and Temperature contours (T/T_∞) in the symmetry plane. It can be observed that the jet issue out into the external flow zone with lower transverse momentum, making the plume boundary to just graze the tip of upper stage flare. There is no flow separation in the upstream cylindrical portion or anywhere on the upper stage due to setting up of benign flow after the jet-upstream flow interaction. Even the Mach disc appeared to be diffused and dragged in the downstream direction. In this test case, the temperature in the base cavity region had almost reached an average of the stagnation temperature of jet and free stream and the zone had been filled with dead air. The streamline pattern is depicted in Fig. 8 shows recirculation bubbles in the region between the plume boundary and the upstream side of the Mach disc. A relatively small recirculation bubble had formed downstream of the Mach disc along the axial direction similar to the 500 mm case. It can be concluded that the flow environment for the 1,000 mm separation

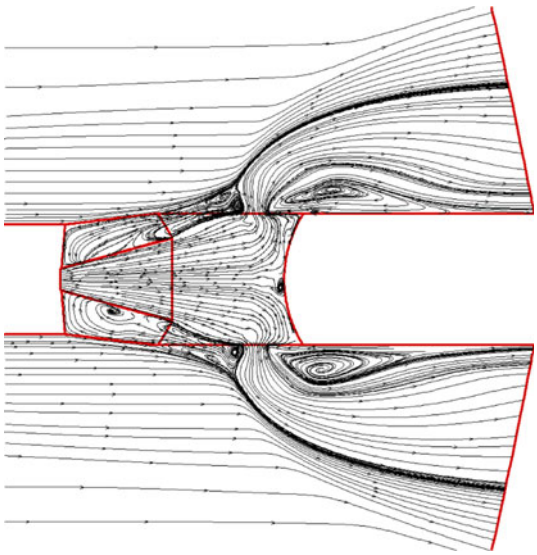

Fig. 8 Zoomed view of streamline pattern for separation distance of 1,000 mm

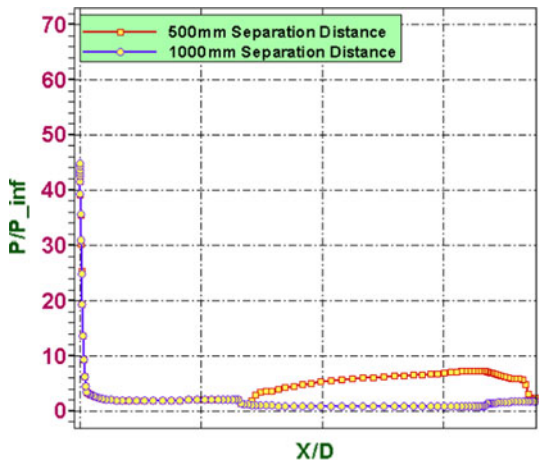

Fig. 9 Comparison of pressure distribution (P/P_∞) for the upper stage of TSR

distance case is very much benign compared to 500 mm separation distance case.

Pressure distribution along the axial direction over the upper stage body surface for both the 500 and 1,000 mm separation distance cases are plotted in Fig. 9. It can be observed that the nose stagnation pressure had reached about 45 times the free stream pressure (P_∞) for both the cases and due to flow expansion further downstream, the pressure had asymptotically reached a value twice the P_∞. However, it is interesting to note that, for the 500 mm case, due to the adverse pressure gradient build up on the cylindrical region, the pressure had increases substantially to about 7 times P_∞. Contrastingly for the 1,000 mm case, the cylindrical portion of the upper-stage had been subjected to sub-atmospheric pressure all through.

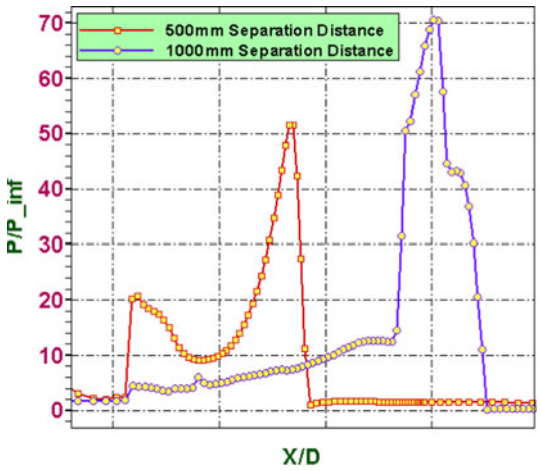

Fig. 10 Comparison of pressure distribution (P/P_∞) on the periphery of inter-stage gap joining the lower and upper stages

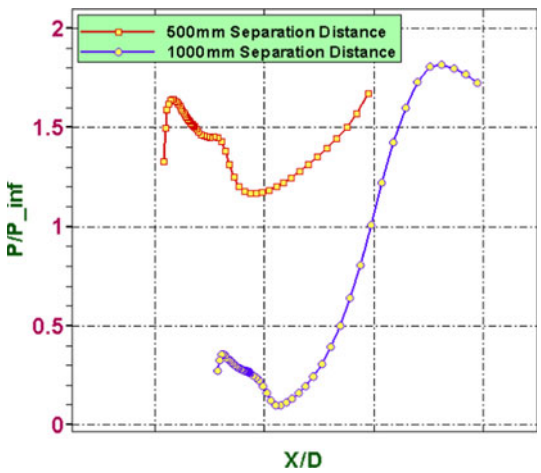

Fig. 11 Comparison of pressure distribution (P/P_∞) for the lower stage of TSR

Figure 10 shows the comparison of pressure distribution along the axial direction on the periphery of inter-stage gap joining the lower and upper stages. It can be observed that the pressure along the inter-stage gap had built-up to about five times P_∞ for the 500 mm case and about 70 times P_∞ for the 1,000 mm case due to the complex Mach disc and the flow squeezing out of the narrow gap. Figure 11 shows the pressure distribution over the lower stage along the axial direction. The static pressure for 500 mm case is higher than the 1,000 mm case and there is a zone of sub-atmospheric pocket for the latter due to large downstream expansion of jet flow over the cylindrical body.

Effect of Order of Spatial Accuracy on the Flow Solution

As mentioned in the previous section, for the 500 mm separation distance case, there is a huge flow separation on the cylindrical portion of the upper stage of the rocket due to the jet-upstream flow interaction. A study was carried out to bring out the effect of order of spatial accuracy of the governing equations on the flow field resolution. For this, the 500 mm case had been considered for analysis and the flow field was evaluated for first order and second order spatial resolution of the RANS equations. The flow field simulated with the first order and the second order spatial accuracies are shown with Mach contours in Figs. 12 and 3, respectively. It is observed that, both the results are found incomparable and the first order accuracy was found inadequate to resolve and capture the physics in any reasonable detail at all. In case of the first order solution, the complex flow which had appeared as large separation bubble over the cylindrical portion for the second order accurate simulation had been found attached to the wall and is unseparated for most of the cylindrical portion except at the trailing edge of the cylindrical regions where a small separation bubble had formed due to the adverse pressure gradient created by the jet cross flow. Also the Mach disc is highly smeared. Since the jet flow is highly inertial (convection dominated), it is necessary to resolve the spatial mean flow quantities to at least second order accuracy. Also, what had been the subsonic portion of the boundary layer in case of the second order accuracy had become supersonic part of boundary layer in the first order accurate case, thereby preventing the jet flow to creep upstream through the boundary layer. This upstream creeping of jet flow into the subsonic portion of the boundary layer only can cause such massive flow separation over the body which is the actual reality. The physical diffusion required near the wall for making a portion of the boundary layer to subsonic speeds from supersonic speeds required accurate representation of the flow variables. The first order solution had in fact conjured the physical reality and diffused the solution to such unacceptable levels where the critical information such as 'stage-separation distance'

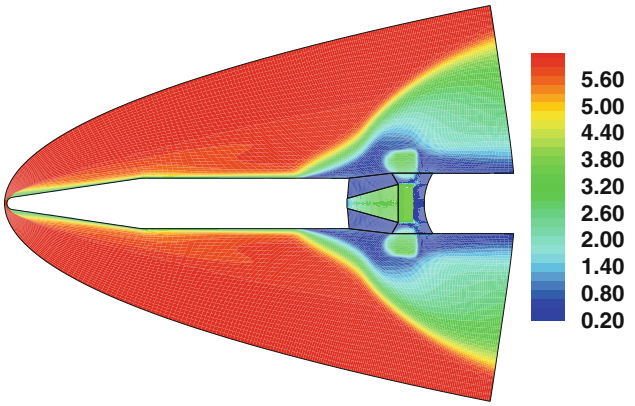

Fig. 12 Mach contours for separation distance of 500 mm with first order spatial resolution

is to be delivered to a designer. Thus it is absolutely necessary to use a blend of low-dissipative numerical schemes in conjunction with a second order of accurate spatial resolution for such critical flows involving massive separations and interactions. Also it has to be recognised that the eddy viscosity models like the Spalart–Allmaras model used in the present study just mimics the turbulent behaviour and does not actually solve for the turbulent fluctuations as simulated using LES or DNS. Hence the above discussions on the stream wise flow separation are restricted within realm of predictive capability of turbulence model.

Conclusions

CFD simulations were carried out to determine the flow field during the jettisoning process of a two stage rocket. Two simulations with stage separation distances of 500 and 1,000 mm were considered for simulation. It had been found from the viscous simulation that the there is a huge jet-upstream interference for the 500 mm case resulting in upstream flow separation. For the 1,000 mm case, the flow is distortion free and the jet simply gets flushed downstream without any adverse interference with the upstream external flow. The flow field for this case is very benign compared to that of 500 mm separation distance case. Due to constant ratio of specific heats ($\gamma = 1.233$) assumption in the present simulations, the estimate of 1,000 mm is conservative. Specific study was carried out on the necessity of using second order accurate flow simulations in case of such complex jet-free stream interactions.

For such complex stage separation scenario it is very difficult to perform wind tunnel experiments considering the fact that the ambient flight condition of TSR is less dense and associated complexities of including the stage separation schemes adds more constraints. Thus, CFD is the only viable option for studying the stage separation of the TSR.

References

1. C. Breitsamter, B. Laschka, C. Zahringert, G. Sachs, Wind tunnel tests for separation dynamics modeling of a two-stage hypersonic vehicle. AIAA/NAL-NASDA-ISAS 10th International space planes and hypersonic systems and technologies conference (AIAA paper 2001-1811), Kyoto, Japan, April 2001
2. W.D. Blocker, P.E, D.E. Reubush, X-43A stage separation system—a flight data evaluation. AIAA/CIRA 13th International space planes and hypersonics systems and technology conference, (AIAA paper 2005-3335)
3. K.J. Murphy, W.I. Scallion, Experimental stage separation tool development in NASA Langley's Aerothermodynamics Laboratory. AIAA atmospheric flight mechanics conference and exhibit (AIAA paper 2005-6127), San Francisco, California, Aug 2005
4. C.E. Lungu, S.G. Ramasamy, D.E. Scarborough, J. Jagoda, S. Menon, Experimental studies of stage separation in a Mach 2.5 free stream. 47th AIAA Aerospace sciences meeting including the new horizons forum and aerospace exposition (AIAA paper 2009-1093), Orlando, Florida, Jan 2009
5. P. Kumar, R. Swaminathan, C. Unnikrishnan, V. Ashok, V. Adimurthy, Modelling of jet impingement forces during hot stage-separation of a launch vehicle. 34th AIAA/ASME/SAE/ASEE joint propulsion conference & exhibit (AIAA paper 98-3156), Cleveland, OH, July 1998
6. P.G. Buning, T.-C. Wong, A.D. Dilley, J.L. Pao, Prediction of hyper-X stage separation aerodynamics using CFD. 18th AIAA applied aerodynamics conference (AIAA paper 2000-4009), Denver, CO, August 2000
7. P. Liever, S. Habchi, W. Engelund, J. Martin, Stage separation analysis of the X-43A research vehicle. 22nd applied aerodynamics conference and exhibit (AIAA paper 2004-4725), Providence, Rhode Island
8. M. Mirzaei, B.N. Nia, A. Shadaram, Numerical simulation of stage separation maneuver with jet interaction. Aircraft Engineering and Aerospace Technology: An International Journal **78**(3), 217–225 (2006)
9. F. Paglia, A. Pizzicaroli, E. Lambiase, C. Contini, C. Dumaz, F. Stella, M. Giangi, D. Barbagallo, Vega launcher aerodynamics at separation of first stage. 43rd AIAA/ASME/SAE/ASEE joint propulsion conference & exhibit (AIAA paper 2007-5859), Cincinnati, OH, July 2007
10. S.J. Zhang and X. Zhao, Computational studies of stage separation with an unstructured Chimera grid method, 43rd AIAA/ASME/SAE/ASEE Joint propulsion conference & exhibit (AIAA paper 2007-5409), July 2007, Cincinnati, OH
11. B.N. Pamadi, J. Pei, J.T. Pin, G.H. Klopfer, S.D. Holland, P.F. Covell, Aerodynamic analyses and database development for Ares I vehicle first stage separation. 49th AIAA Aerospace sciences meeting including the new horizons forum and aerospace exposition (AIAA paper 2011-0171), Orlando, Florida, January 2011
12. E. Kless, H.C. Lee, G.H. Klopfer, J.T. Onufer, Validation of OVERFLOW for computing plume effects during the ares 1 stage separation process. 49th AIAA aerospace sciences meeting (AIAA paper 2011-170), Orlando, Florida, January 2011
13. Y. Wang, H. Ozawa, H. Koyama and Y. Nakamura, Simulation of supersonic stage separation of capsule-shaped abort system by aerodynamic interaction. 20th AIAA computational fluid dynamics conference (AIAA paper 2011-3064), Honolulu, Hawaii, June 2011
14. R. Balasubramanian, K. Anandhanarayanan, Indigenous development of compressible Reynolds averaged Navier-Stokes solver, CERANS, DRDO science spectrum, (DESIDOC, Ministry of Defence, DRDO, New Delhi, 2009), pp. 219–226
15. K. Anandhanarayanan, R. Balasubramanian, A multiblock approach for simulating control surface deflections of a hypersonic vehicle. Journal of Aerospace Quality and Reliability **1**(2), 61–66 (2005)
16. R. Balasubramanian, K. Anandhanarayanan, Viscous computations for complex flight vehicles using CERANS with wall function. Proc. of the SAROD-2005, Hyderabad, India, Dec 2005